LUPINE PUBLISHERS

Open Access Journal of Biomedical Engineering and Biosciences

DOI: 10.32474/OAJBEB.2019.03.000163

ISSN: 2637-4579

Research Article

Evaluation of the Physicochemical and Thermal Properties of Antimony: Influence of the Energy of Consciousness Healing Treatment

Dahryn Trivedi[1], Mahendra Kumar Trivedi[1], Alice Branton[1], Gopal Nayak[1], Snehasis Jana[2]*

[1]*Trivedi Global, Inc., Henderson, USA*

[2]*Trivedi Science Research Laboratory Pvt. Ltd, Thane, India*

***Corresponding author:** Snehasis Jana, Trivedi Science Research Laboratory Pvt. Ltd, Thane (W), Maharashtra, India

Received: June 06, 2018 **Published:** June 27, 2018

Abstract

Antimony and its compounds are mainly used in the preparation of paints, flame-proofing materials, ceramic enamels, pottery, and glass as well as in the treatment of leishmaniasis. This study analyzes the effect of the Trivedi Effect®-Consciousness Energy Healing Treatment on the physicochemical and thermal properties of antimony in comparison to the untreated sample. The sample was divided into control and treated parts. The control part has not received any treatment; while the treated part was received the Trivedi Effect®-Consciousness Energy Healing Treatment by a renowned Biofield Energy Healer, Dahryn Trivedi, remotely. The particle size distribution of the treated antimony powder at d_{10}, d_{50}, d_{90}, and D (4,3) was significantly altered by 4.05%, -1.40%, 11.92%, and 7.69%, respectively, compared to the control sample. Therefore, the treated sample showed a significant decrease in the specific surface area by 20.24% than the control sample. The powder X-ray diffraction peak intensities of the treated sample altered ranging from -58.50% to 10.38%; while the crystallite sizes were reduced ranging from of 14.07% to 48.70% compared with the control sample. The average crystallite size of the treated sample was also significantly reduced by 28.90%, compared to the control sample. The total weight loss was decreased during thermal degradation of the treated sample by 2.68%; however, the residue weight was significantly increased by 8.75% compared to the control sample. The maximum thermal degradation temperature was significantly increased in the treated sample by 11.49% (~60ºC) compared to the control sample. The overall study indicated the reduced surface area, altered crystalline properties, and improved thermal stability of the antimony sample after the Trivedi Effect®-Consciousness Energy Healing Treatment. Therefore, the Biofield Energy Treatment could be considered as a novel approach for generating a new polymorph of antimony that might help in improving its appearance, bioavailability, flowability, and thermal stability in comparison to the untreated sample. The Biofield Energy Treated antimony might be proved as beneficial in developing more efficacious nutraceutical/pharmaceutical formulations as well as in the heavy industries for the production of alloys, fire retardant, solders, electrical cables, microelectronics, bullets, plain bearings, etc.

Keywords: Antimony; Consciousness Energy Healing Treatment; The Trivedi Effect®; Particle Size; Crystallite Size; Weight Loss

Introduction

Antimony (Sb) is a silvery white metal in appearance and its compounds are mainly used in the preparation of paints, flame-proofing materials, ceramic enamels, pottery, and glass. However, its compounds have also been used medically after they were introduced in the 14th century by the alchemist John of Rupescissa [1]. The antimony compounds have main pharmacological use in the treatment of the parasitic diseases, leishmaniasis, and schistosomiasis. In 1631, the compound of antimony, potassium antimony tartrate, has been introduced by the German alchemist, Adrian Von Mynsicht; however, after that, the antimony compounds lost their value due to their toxic properties [2]. Later on, during 1918-1920, the interest in such compounds revived after the establishment of the medicinal value of tartar emetic by Christopherson and Rogers [3]. Since then, the antimony compounds have been used for the treatment of schistosomiasis and leishmaniasis. The examples of antimony compounds used in the treatment of schistosomiasis include sodium antimony dimercaptosuccinate, sodium antimony tartrate (astiban, stibocaptate), and sodium antimonyl gluconate, etc. [4,5]. Nowadays, the medicinal use of antimonials has been largely

restricted to the treatment of leishmaniasis [6,7]. The antimony compounds that have been used in chemotherapy can be broadly divided into two classes:

a) carbon-antimony bond containing compound such as 4-acetylaminobenzenestibonic acid (Stib-acetin) and 4-aminobenzenestibonic acid (Stibamin);

b) antimony-oxygen or antimony-sulphur bonds containing compounds that further form an antimoniate ester.

The examples of such compounds included the trivalent and pentavalent antimonials, e.g., triostam, meglumine antimonate (glucantime), pentostam, stibocaptate, urea stibamine, stibophen, sodium antimony dimethylcystein, and MSb B, etc. [8]. Besides, the use of antimonials has also been evident as emetics [9]. The antimony compounds are also used in various veterinary preparations as a skin conditioner in ruminants, e.g., lithium antimony thiomalate and anthiomaline. It has a nourishing effect on the keratinized tissues in animals [10]. It was also reported that the compounds of Sb (III) might show antitumor activities with amino polydentate carboxylic acids for some metal ions coordinates such as, O, Ba, Bi, Co, Mn, Cu, Ni, Sn, Pb, and Zn [11]. The scientific studies reported that the in vivo application of such compounds showed an increase in the life span of mice induced with Ehrlich ascites tumour and spindle sarcoma [12,13]. The ADME profile of any drug has been decided mainly by its physicochemical properties such as melting point, solubility, partition coefficient, and crystalline properties, etc. play Thus, the scientific researches these days focus those approaches that might help in enhancing the efficacy and biological activities of drug by altering the physicochemical properties [14]. The Consciousness Energy Healing Treatment is such kind of approach that is used these days to modify the physicochemical, crystalline, and thermal properties of drugs for improving their role in the body [15-18]. The concept of Biofield Energy Healing is widely accepted as an alternative integrative approach due to its ability to correct the root cause of the diseases and thereby improve the quality of life [19-21]. In the same manner, the Trivedi Effect®- Consciousness Energy Healing Treatment has also been reported for its beneficial impact in various fields. A human has the ability to transmit the energy to any living organism(s) or nonliving object(s) around the globe by harnessing it from the universe. The object or recipient that receives the energy always responds in a useful way. This process is known as the Trivedi Effect® - Biofield Energy Healing Treatment [22,23]. Various research studies reported the beneficial impact of The Biofield Energy Treatment in the field of biotechnology [24,25], antimicrobial activity [26-28], nutraceuticals [29,30], agriculture and productivity [31,32], bone health [33], cancer research [34], skin health [35], and metals, chemicals, ceramics and polymers [36-38], etc. This study has the objective to establish the impact of the Trivedi Effect® on the physicochemical and thermal properties of antimony by using various analytical techniques.

Materials and Methods

Chemicals and Reagents

The test sample antimony was purchased from Parshwamani Metals, Mumbai, Maharashtra, India and the other chemicals used in the experiments were purchased in India.

Consciousness Energy Healing Treatment Strategies

The antimony sample used in the study was first divided into two parts. The first part of sample was not received the Biofield Energy Treatment and considered as the control sample. Besides, the second part of sample was received the Trivedi Effect®-Energy of Consciousness Healing Treatment under standard laboratory conditions for 3 minutes and known as the treated antimony sample. This Biofield Energy Treatment was provided remotely through the healer's unique energy transmission process by the well-known Biofield Energy Healer, Dahryn Trivedi, USA, to the test sample. Later on, the control sample was treated with a "sham" healer for comparison purpose, who did not have any awareness about the Biofield Energy Treatment. Finally, both the samples were kept in sealed conditions and characterized using PSA, PXRD, and TGA/DTG analytical techniques.

Characterization

The particle size distribution (PSD) analysis of antimony powder was performed with the help of Malvern Mastersizer 2000 (UK) using the wet method [39,40]. The powder X-ray diffraction (PXRD) analysis of antimony powder also performed with the help of Rigaku MiniFlex-II Desktop X-ray diffractometer (Japan) [41,42]. The crystallites size was calculated using the Scherrer's formula (1)

$$G = k\lambda/\beta\cos\theta \quad (1)$$

Where G is the crystallite size in nm, k is the equipment constant, β is the full-width at half maximum, λ is the radiation wavelength, and θ is the Bragg angle [43]. Similarly, the thermal gravimetric analysis (TGA) of antimony powder was performed with the help of TGA Q50 TA instruments [44]. The % change in specific surface area, particle size, crystallite size, peak intensity, weight loss and the maximum thermal degradation temperature of the treated antimony powder was calculated compared with the control sample using the following equation 2:

$$\%\ \text{change} = [(\text{Treated} - \text{Control})/\text{Control}] \times 100 \quad (2)$$

Results and Discussion

Particle Size Analysis (Psa)

The impact of the Biofield Energy Treatment on the particle size distribution and surface area of antimony powder were performed and the results were compared with the particle size data of the control sample (Table 1). The particle sizes at d_{10}, d_{90}, and d (4, 3) of the treated sample were observed to increase by

4.05%, 11.92%, and 7.69%, respectively; while the particle size at d_{50} was slightly reduced by 1.40%, as compared to the control sample. The significant increase in the particle size resulted in the reduced surface area of the treated sample by 20.24% after the Biofield Energy Treatment, in comparison to the control sample. It was previously reported that the particle sizes of compounds might increase after increasing the thermal energy. Thus, it could be assumed that the Biofield Energy Treatment might increase the thermal energy within the molecules of antimony sample, which helps in decreasing the nucleus densities and thereby resulted in the increased particle size [45,46]. Besides, the increased particle size might be associated with the improved shape, flowability, appearance, and compactibility [47,48] of the treated sample as compared to the control sample.

Table 1: Particle size distribution of the control and treated antimony.

Parameter	d_{10}(µm)	d_{50} (µm)	d_{90} (µm)	D (4,3) (µm)	SSA(m^2/g)
Control	3.7	14.95	63.42	25.62	0.84
Biofield Treated	3.85	14.74	70.98	27.59	0.67
Percent change (%)	4.05	-1.4	11.92	7.69	-20.24

Powder X-Ray Diffraction (PXRD) Analysis

The PXRD analysis was done in both the samples and the corresponding diffractograms are presented in (Figure 1). The diffractogram of the control and treated sample showed sharp and intense peaks that indicated their crystalline nature. The further study analyses the changes in the intensities of peaks, and the corresponding crystallite sizes between the control and treated sample (Table 2). The treated sample showed significant changes in the peak intensities and corresponding crystallite sizes. The intensities of the treated sample were altered ranging from -58.50% to 10.38%; while the crystallite sizes were decreased ranging from 14.07% to 48.70%, as compared to the control sample. Also, the treated sample showed a significant reduction in the average crystallite size (290.63 nm) by 28.90% in comparison to the control sample (408.75 nm). The significant alteration in the intensities and crystallite size indicated the altered crystalline structure and morphology of drug that might be possible due to the new polymorph generation of antimony powder [49,50] after the Biofield Energy Treatment. Moreover, it was reported that the polymorphic form of the compound might be helpful in improving the bioavailability and efficacy profile of the drug [51]. Therefore, the treated sample might show better bioavailability and efficacy than the control sample.

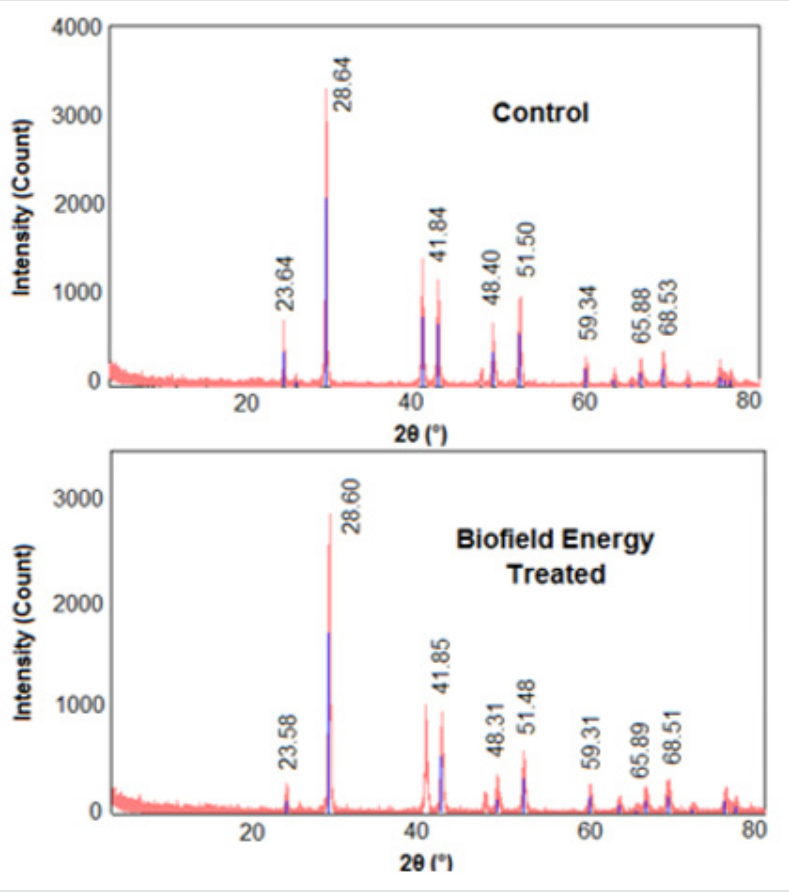

Figure 1: PXRD diffractograms of the control and treated antimony.

Table 2: PXRD data for the control and treated antimony.

Entry No.	Bragg angle (°2θ)		Intensity (cps)			Crystallite size (G, nm)		
	Control	Treated	Control	Treated	% Change	Control	Treated	% Change
1	23.64	23.58	80	33.2	-58.5	509	325	-36.15
2	28.64	28.6	496	536	8.06	465	329	-29.25
3	41.84	41.85	221	203	-8.14	356	290	-18.54
4	48.4	48.31	126	66	-47.62	423	217	-48.7
5	51.5	51.48	207	135	-34.78	327	281	-14.07
6	59.34	59.31	47.2	52.1	10.38	519	377	-27.36
7	65.88	65.89	53	55	3.77	326	263	-19.33
8	68.53	68.51	68	70	2.94	345	243	-29.57

Thermal Gravimetric Analysis (TGA)/ Differential Thermogravimetric Analysis (DTG)

The TGA/DTG technique helps in establishing the thermal degradation and stability profile of the sample. In this study, this technique helps in analysing the difference in the thermal stability profile of the treated sample compared to the control sample. The TGA thermograms (Figure 2) of the control and treated samples showed significant weight loss during their thermal degradation. The data indicated that the total weight loss of the treated sample was reduced by 2.68% after the Biofield Energy Treatment in comparison to the control sample (Table 3). Such a reduction in the weight loss signifies the increase in the residue weight of the treated sample by 8.75% after the thermal degradation, compared to the control sample. Such changes in the thermal degradation pattern might be attributed to the significant increase in the particle size of the treated sample after the Biofield Energy Treatment as the large sized particles might reduce the thermal degradation, compared to the control sample [52]. The DTG thermograms of both the samples, i.e., the control and treated samples were showed a single peak in both the thermograms (Figure 3). The peak present in the thermograms of both the samples (T_{max}) denoted the temperature at which maximum thermal degradation has taken place. The results revealed that the Tmax of the treated sample was significantly increased by 11.49% (~60°C) as compared to the control sample. Hence, it could be suggested that the thermal degradation of the treated sample was reduced after the Biofield Energy Treatment in comparison to the control sample. Thus, the overall analysis indicated the improved thermal stability profile of the treated sample as compared to the untreated sample. It would be more important in the pharmaceutical industry as well as in the heavy industries for the production of alloys, fire retardant, solders, electrical cables, microelectronics, bullets, plain bearings, etc.

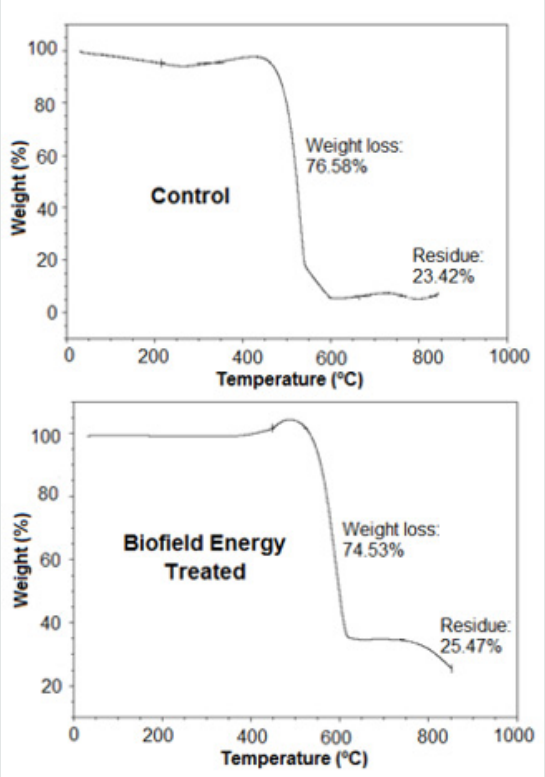

Figure 2: TGA thermograms of the control and treated antimony.

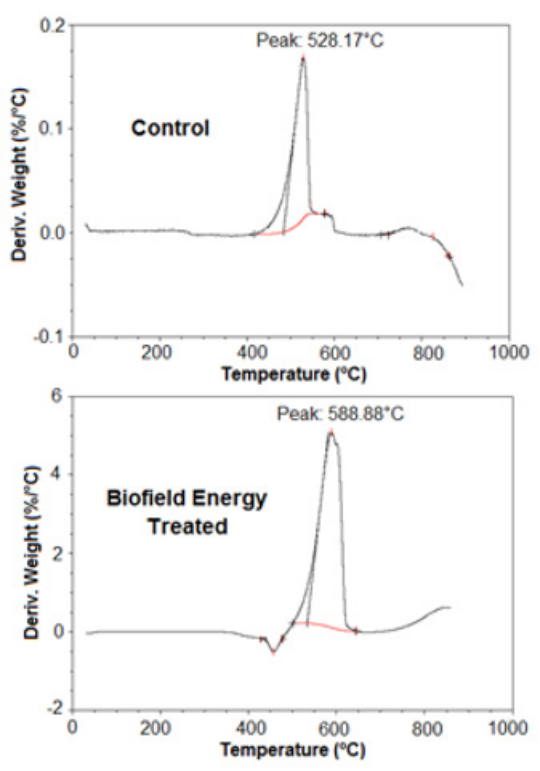

Figure 3: DTG thermograms of the control and Biofield Energy Treated antimony.

Table 3: TGA/DTG data of the control and treated samples of antimony.

Sample	TGA		DTG
	Total Weight Loss (%)	Residue %	T_{max} (°C)
Control	76.58	23.42	528.17
Biofield Energy Treated	74.53	25.47	588.88
% Change	-2.68	8.75	11.49

T_{max} = the temperature at which maximum weight loss takes place in TG or peak temperature in DTG.

Conclusion

In this study, the Trivedi Effect®-Consciousness Energy Healing Treatment has been shown its significant impact on the physicochemical and thermal properties of antimony sample in comparison to the untreated sample. The particle size distribution of the Biofield Energy Treated antimony powder at d_{10}, d_{50}, d_{90}, and D (4,3) was significantly altered by 4.05%, -1.40%, 11.92%, and 7.69%, respectively, compared to the control sample. Therefore, the Biofield Energy Treated sample showed a significant decrease in the specific surface area by 20.24% than the control sample. The powder X-ray diffraction peak intensities of the Biofield Energy Treated sample altered ranging from -58.50% to 10.38%; while the crystallite sizes were reduced ranging from of 14.07% to 48.70% compared with the control sample. The average crystallite size of the Biofield Energy Treated sample was also significantly reduced by 28.90%, compared to the control sample. The total weight loss was decreased during thermal degradation of the Biofield Energy Treated sample by 2.68%; however, the residue weight was significantly increased by 8.75% compared to the control sample. The maximum thermal degradation temperature was significantly increased in the Biofield Energy Treated sample by 11.49% (~60ºC) compared to the control sample. Hence, the overall study indicated the significant impact of the Trivedi Effect®-Consciousness Energy Healing Treatment on the antimony powder that might form a novel polymorph of antimony with improved appearance, compatibility, and flowability along with increased thermal stability as compared to the control antimony sample. Thus, the Biofield Energy Treated antimony could be used in the novel pharmaceutical/ nutraceutical preparations with improved performance and efficacy profile for the treatment of disorders such as leishmaniasis, and other uses such as emetics, veterinary preparations, skin conditioner in ruminants, and anti-tumor agent, etc. Besides, it can be more useful in heavy industries for the production of alloys, fire retardant, solders, electrical cables, microelectronics, bullets, plain bearings, etc.

Acknowledgement

The authors are grateful to Central Leather Research Institute, SIPRA Lab. Ltd., Trivedi Science, Trivedi Global, Inc., Trivedi Testimonials, and Trivedi Master Wellness for their assistance and support during this work.

References

1. McCallum, Robert lan (1999) Antimony in Medical History. The Pentland Press, Edinburgh, UK.
2. Sneader W (2005) Drug Discovery: A History. John Wiley & Sons, West Susssex, UK.
3. Sundar S, Chakravarty J (2010) Antimony toxicity. Int J Environ Res Public Health 7: 4267-4277.
4. Farid Z, Bassily S, Kent DC, Hassan A, Abdel-Wahab MF, et al. (1968) Urinary schistosomiasis treated with sodium antimony tartrate a quantitative evaluation. Brit Med J 3: 713-714.
5. Davis A (1968) Comparative trials of antimonial drugs on urinary schistosomiasis. Bull World Health Organ 38: 197-227.
6. Brito NC, Rabello A, Cota GF (2017) Efficacy of pentavalent antimoniate intralesional infiltration therapy for cutaneous leishmaniasis: A systematic review. PLoS One 12: 0184777.
7. Nunes DCO, Bispo-da-Silva LB, Napolitano DR, Costa MS, Figueira MMNR, et al. (2017) In vitro additive interaction between ketoconazole and antimony against intramacrophage Leishmania (Leishmania) amazonensis amastigotes. PLoS One 12: e0180530.
8. Sharma S, Anand N (1997) Organometaliics. Pharmacochemistry Library, Elsevier.
9. Russell CA (2000) Antimony's Curious History. Notes and Records of the Royal Society of London 54: 115-116.
10. Kassirsky IA, Plotnikov NN (2003) Diseases of Warm Lands: A Clinical Manual. University Press of the Pacific Honolulu, Hawaii.
11. Sharma P, Perez D, Cabrera A, Rosas N, Arias JL (2008) Perspectives of antimony compounds in oncology. Acta Pharmacol Sin 29: 881-890.
12. Tiekink ERT (2002) Antimony and Bismuth Compounds in Oncology. Critical Reviews in Oncology/Hematology 42: 217-224.
13. Yadav RNP (2012) Metals in Oncology: An Overview. Academic Voices 2: 54-58.
14. Khadka P, Ro J, Kim H, Kim I, Kim JT, et al. (2014) Pharmaceutical particle technologies: An approach to improve drug solubility, dissolution and bioavailability. Asian J Pharm 9: 304-316.
15. Trivedi MK, Branton A, Trivedi D, Shettigar H, Bairwa K, et al. (2015) Fourier transform infrared and ultraviolet-visible spectroscopic characterization of biofield treated salicylic acid and sparfloxacin. Nat Prod Chem Res 3: 186.
16. Trivedi MK, Tallapragada RM, Branton A, Trivedi D, Nayak G, et al. (2015) The potential impact of biofield energy treatment on the atomic and physical properties of antimony tin oxide nanopowder. American Journal of Optics and Photonics 3: 123-128.
17. Branton A, Jana S (2017) The influence of energy of consciousness healing treatment on low bioavailable resveratrol in male Sprague Dawley rats. International Journal of Clinical and Developmental Anatomy 3: 9-15.
18. Branton A, Jana S (2017) The use of novel and unique biofield energy healing treatment for the improvement of poorly bioavailable compound, berberine in male Sprague Dawley rats. American Journal of Clinical and Experimental Medicine 5: 138-144.
19. Warber SL, Cornelio D, Straughn J, Kile G (2004) Biofield energy healing from the inside. J Altern Complement Med 10: 1107-1113.
20. Hammerschlag R, Levin M, McCraty R, Bat N, Ives JA, et al. (2015) Biofield Physiology: A Framework for an Emerging Discipline. Glob Adv Health Med 4: 35-41.
21. Koithan M (2009) Introducing complementary and alternative therapies. J Nurse Pract 5: 18-20.
22. Trivedi MK, Tallapragada RM, Branton A, Trivedi D, Nayak G, et al. (2015) Spectral and thermal properties of biofield energy treated cotton. American Journal of Energy Engineering. 3: 86-92.
23. Trivedi MK, Patil S, Shettigar H, Bairwa K, Jana S (2015) Effect of biofield treatment on spectral properties of paracetamol and piroxicam. Chem Sci J 6: 98.
24. Trivedi MK, Patil S, Shettigar H, Bairwa K, Jana S (2015) Phenotypic and biotypic characterization of Klebsiella oxytoca: An impact of biofield treatment. J MicrobBiochemTechnol 7: 203-206.
25. Nayak G, Altekar N (2015) Effect of biofield treatment on plant growth and adaptation. J Environ Health Sci 1: 1-9.
26. Trivedi MK, Branton A, Trivedi D, Nayak G, Charan S, et al. (2015) Phenotyping and 16S rDNA analysis after biofield treatment on Citrobacter braakii: A urinary pathogen. J Clin Med Genom 3: 129.
27. Trivedi MK, Patil S, Shettigar H, Mondal SC, Jana S (2015) Evaluation of biofield modality on viral load of Hepatitis B and C viruses. J Antivir Antiretrovir 7: 83-88.
28. Trivedi MK, Patil S, Shettigar H, Mondal SC, Jana S (2015) An impact of biofield treatment: Antimycobacterial susceptibility potential using BACTEC 460/MGIT-TB System. Mycobact Dis 5: 189.
29. Trivedi MK, Branton A, Trivedi D, Nayak G, Plikerd WD, et al. (2017) A Systematic study of the biofield energy healing treatment on physicochemical, thermal, structural, and behavioral properties of magnesium gluconate. International Journal of Bioorganic Chemistry 2: 135-145.
30. Trivedi MK, Branton A, Trivedi D, Nayak G, Plikerd WD, et al. (2017) Chromatographic and spectroscopic characterization of the consciousness energy healing treated Withania Somnifera (ashwagandha) root extract. European Journal of Biophysics 5: 38-47.
31. Trivedi MK, Branton A, Trivedi D, Nayak G, Mondal SC, et al. (2015) Morphological characterization, quality, yield and DNA fingerprinting of biofield energy treated alphonso mango (Mangiferaindica L.). Journal of Food and Nutrition Sciences 3: 245-250.
32. Trivedi MK, Branton A, Trivedi D, Nayak G, Mondal SC, et al. (2015) Evaluation of biochemical marker – Glutathione and DNA fingerprinting of biofield energy treated Oryza sativa. American Journal of BioScience 3: 243-248.
33. Koster DA, Trivedi MK, Branton A, Trivedi D, Nayak G, et al. (2018) Evaluation of biofield energy treated vitamin D3 on bone health parameters in human bone osteosarcoma cells (MG-63). Biochemistry and Molecular Biology 3: 6-14.
34. Trivedi MK, Patil S, Shettigar H, Gangwar M, Jana S (2015) In vitro evaluation of biofield treatment on cancer biomarkers involved in endometrial and prostate cancer cell lines. J Cancer SciTher 7: 253-257.
35. Kinney JP, Trivedi MK, Branton A, Trivedi D, Nayak G, et al. (2017) Overall skin health potential of the biofield energy healing based herbomineral formulation using various skin parameters. American Journal of Life Sciences 5: 65-74.
36. Trivedi MK, Tallapragada RM (2008) A transcendental to changing metal powder characteristics. Met Powder Rep 63: 22-28, 31.
37. Trivedi MK, Nayak G, Patil S, Tallapragada RM, Latiyal O (2015) Studies of the atomic and crystalline characteristics of ceramic oxide nano powders after bio field treatment. Ind Eng Manage 4: 161.
38. Trivedi MK, Nayak G, Patil S, Tallapragada RM, Latiyal O, et al. (2015) Effect of biofield energy treatment on physical and structural properties of calcium carbide and praseodymium oxide. International Journal of Materials Science and Applications 4: 390-395.
39. Trivedi MK, Sethi KK, Panda P, Jana S (2017) Physicochemical, thermal and spectroscopic characterization of sodium selenate using XRD, PSD,

DSC, TGA/DTG, UV-vis, and FT-IR. Marmara Pharmaceutical Journal 21/2: 311-318.

40. Trivedi MK, Sethi KK, Panda P, Jana S (2017) A comprehensive physicochemical, thermal, and spectroscopic characterization of zinc (II) chloride using X-ray diffraction, particle size distribution, differential scanning calorimetry, thermogravimetric analysis/ differential thermogravimetric analysis, ultraviolet-visible, and Fourier transform-infrared spectroscopy. International Journal of Pharmaceutical Investigation 7: 33-40.

41. Zhang T, Paluch K, Scalabrino G, Frankish N, Healy AM, et al. (2015) Molecular structure studies of (1S,2S)-2-benzyl-2,3-dihydro-2-(1Hinden-2-yl)-1H-inden-1-ol. J Mol Struct 1083: 286-299.

42. Desktop X-ray Diffractometer "MiniFlex+". The Rigaku Journal 14: 29-36, 1997.

43. Langford JI, Wilson AJC (1978) Scherrer after sixty years: A survey and some new results in the determination of crystallite size. J Appl Cryst 11: 102-113.

44. Trivedi MK, Branton A, Trivedi D, Nayak G, Plikerd WD, et al. (2017) A systematic study of the biofield energy healing treatment on physicochemical, thermal, structural, and behavioral properties of iron sulphate. International Journal of Bioorganic Chemistry. 2: 135-145.

45. Katayama M (1956) The crystal structure of an unstable form of chloroacetamide. Acta Crystallogr 9: 986-991.

46. Rashidi AM, Amadeh A (2009) The effect of saccharin addition and bath temperature on the grain size of nanocrystalline nickel coatings. Surf Coat Technol 204: 353-358.

47. Buckton G, Beezer AE (1992) The relationship between particle size and solubility. Int J Pharmaceutics 82: 7-10.

48. Mosharrof M, Nystrom C (1995) The effect of particle size and shape on the surface specific dissolution rate of microsized practically insoluble drugs. Int J Pharm 122: 35-47.

49. Trivedi MK, Branton A, Trivedi D, Nayak G, Plikerd WD, et al. (2017) Evaluation of the physicochemical, spectral, thermal and behavioral properties of sodium selenate: influence of the energy of consciousness healing treatment. American Journal of Quantum Chemistry and Molecular Spectroscopy 2: 18-27.

50. Trivedi MK, Branton A, Trivedi D, Nayak G, Lee AC, et al. (2017) Evaluation of the impact of biofield energy healing treatment (the Trivedi Effect®) on the physicochemical, thermal, structural, and behavioural properties of magnesium gluconate. International Journal of Nutrition and Food Sciences 6: 71-82.

51. Junyaprasert VB, Morakul B (2015) Nanocrystals for enhancement of oral bioavailability of poorly water-soluble drugs. Asian J Pharm 10: 13-23.

52. Sovizi MR, Hajimirsadeghi SS, Naderizadeh B (2009) Effect of particle size on thermal decomposition of nitrocellulose. J Hazard Mater 168: 1134-1139.

DOI: 10.32474/OAJBEB.2019.03.000163